Sustainable Processes Connect
2025, Vol. 1, Issue 1, Cite as: doi:10.x/journal.x.x.x

SCIFINITI PUBLISHING

OPEN ACCESS

Review Article

Organic Compounds Removal using Magnetic Biochar from Textile Industries based Wastewater-A Comprehensive Review

Avanish Kumar, Ashish Kapoor, Amit Kumar Rathoure, G.L. Devnani, Dan Bahadur Pal*

Department of Chemical Engineering, Harcourt Butler Technical University Kanpur Uttar Pradesh, India

***Corresponding Author:** dbpal@hbtu.ac.in

Abstract

Textile industries are among the largest contributors to global water pollution, discharging wastewater laden with dyes, heavy metals, and synthetic chemicals that pose serious environmental and health threats. Conventional treatment methods often fall short in effectively removing these pollutants and are hindered by high operational costs, sludge production, and limited reusability. In this context, magnetic biochar has emerged as a promising, sustainable, and cost-effective material for textile wastewater remediation. This review explores the synthesis strategies of magnetic biochar—primarily focusing on co-precipitation and iron precursor pyrolysis methods—along with their key physicochemical and magnetic characteristics assessed through XRD, SEM, BET, FTIR, and VSM analyses. The adsorption behaviour of magnetic biochar is further discussed through isotherm and kinetic models, such as Langmuir, Freundlich, pseudo-second-order, and intra-particle diffusion models. The mechanisms driving pollutant removal include electrostatic attraction, pore filling, π–π interactions, and catalytic Fenton-like reactions. Case studies on dye and heavy metal removal demonstrate the material's high efficiency, ease of recovery, and reusability. Finally, the paper highlights current research gaps, scalability issues, and future prospects for advancing magnetic biochar technologies in industrial-scale wastewater treatment. This review provides a comprehensive understanding to guide future innovations and practical applications in sustainable water management.

Keyword: magnetic biochar; co-precipitation; pyrolysis; regeneration; vibrating sample magnetometry; biological oxygen demand

Graphical Abstract

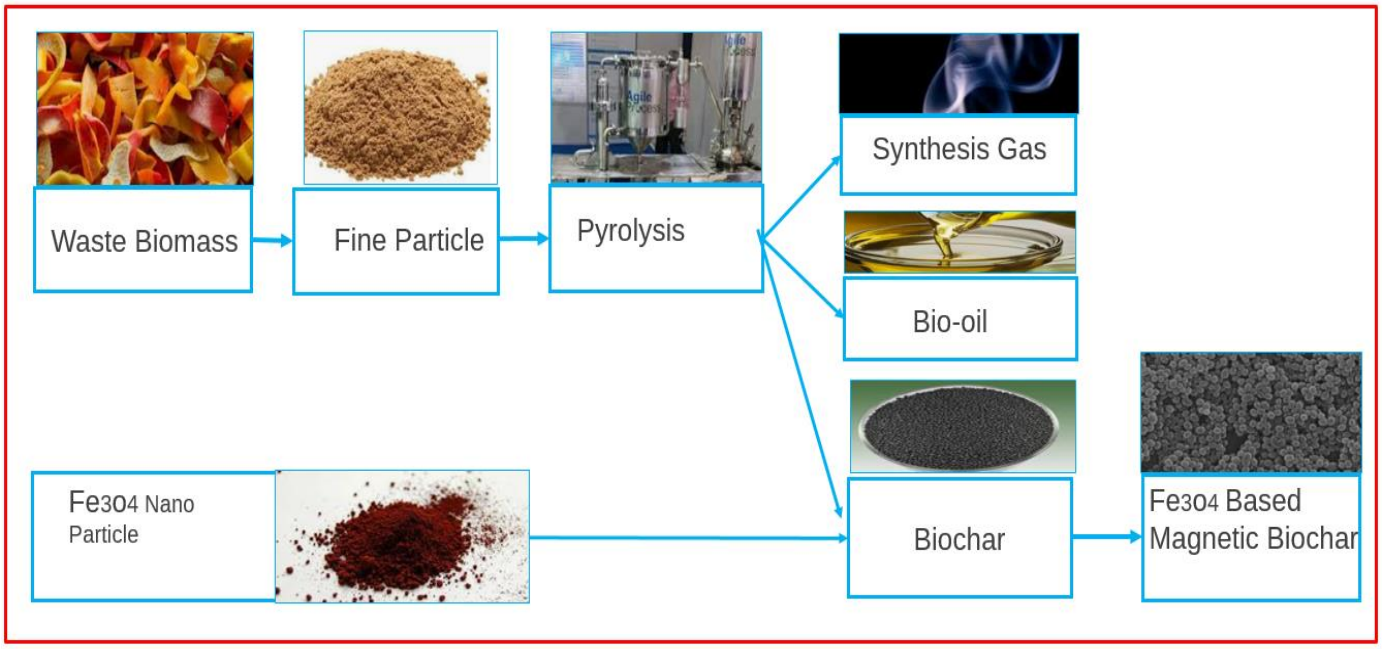

Highlights:

- Organic Compounds Removal using Magnetic Biochar from Textile Industries Wastewater
- Methods used conventional treatment methods economic and cost-effective adsorbents
- Adsorption isotherm and kinetic models for Magnetic Biochar from Textile Industries Wastewater
- Adsorption mechanisms of magnetic biochar adsorbent like pore filling, π–π interactions etc.

1. Introduction

Water is one of the most essential natural resources for life on Earth but the readily available and safe for human consumption is remarkably small. The Earth is often referred to as the "blue planet" because about 71% of its surface is covered with water [1]. However, a closer examination reveals that only a tiny fraction of this water is accessible for direct human use. Approximately 97.5% of the total water on Earth is saline,

found in oceans and seas, and is not suitable for drinking, irrigation, or most industrial purposes without undergoing expensive desalination processes [2]. This leaves only 2.5% of the Earth's water as freshwater, which could, in principle, support human needs. However, this freshwater is not entirely within reach. A significant portion of it about 68.7% is locked away in glaciers and ice caps, primarily in Antarctica and Greenland [3]. Another 30.1% is stored underground in aquifers, some of which are deep and not easily accessible or renewable [4]. That leaves just a small fraction around 1.2% of the total freshwater available in surface water bodies such as rivers, lakes, and swamps. As it well known that only 0.007% water is consumable in total fresh water available as 0.03%in planet volume of water [5]. This small quantity of the water needs for drinking, sanitation, agriculture, industry, and ecosystem maintenance. So as per population growth, urbanization, industrial development, the freshwater availability is becoming a serious issue, and the imbalance between supply and demand is leading to water shortage, degraded water quality which are require to manage more urgent than ever. In modern time water pollution is one of the most serious problems worldwide, arising from both domestic and industrial sources [6] Industrial wastewater is in complex composition and contain toxic pollutants. The textile industries are known for its high-water consumption and discharge of chemically loaded wastewater in to river [7]. The released water into rivers, lakes, or the ground, causing severe harm to aquatic life and posturing risks to human health [8]. Because the textile wastewater is a highly toxic due to containing dyes, surfactants, salts, heavy metals (like chromium, copper, and zinc), and organic chemicals [9]. During processes like dyeing, washing, and bleaching, a significant portion of the used chemicals are not fixed onto the fabric and are instead released into wastewater streams. Dyes, particularly synthetic and azo dyes, are resistant to degradation and can remain in water bodies for extended periods, obstructing sunlight penetration and disrupting photosynthetic activity in aquatic plants [10]. The high biological and chemical oxygen demand (BOD and COD) of textile wastewater also depletes dissolved oxygen in water and threatening aquatic organisms [11]. Although Conventional wastewater treatment methods such as coagulation-flocculation, activated sludge processes, and membrane filtration have been widely employed to manage textile effluents [12]. While these methods can reduce pollutant loads to some extent, they often fall short in completely removing synthetic dyes and trace heavy metals. Moreover, these technologies are energy-intensive, generate secondary sludge that requires further treatment, and are expensive to operate and maintain, particularly for small to medium-scale textile units in developing countries. The inefficiency in dealing with non-biodegradable organic pollutants and the economic burden of advanced methods like reverse osmosis or advanced oxidation processes further highlight the need for more sustainable and cost-effective alternatives [13]. In recent years, biochar produced through the pyrolysis of biomass has emerged as a promising adsorbent for wastewater treatment [14]. Due to its porous structure, large surface area, and abundant surface functional groups, biochar can effectively adsorb a wide range of

pollutants, including dyes, heavy metals, and organic compounds. Moreover, biochar is eco-friendly, inexpensive, and can be derived from agricultural waste such as water hyacinth, rice husk, or coconut shells, and other biomass which are using to prepare biochar and again treated with Fe_3O_4 where magnetic biochar is prepared by impregnation and pyrolysis with iron precursors and co- precipitation method. Here twenty important biomass is taken as sense to take revive to understand the behaviour of bioadsorbent in term of their adsorption capacity or removal efficiency. To enhance its performance, biochar is often modified with magnetic particles like iron oxide, resulting in magnetic biochar. This composite not only improves pollutant removal efficiency through combined adsorption and catalytic degradation but also facilitates easy recovery and reuse using magnetic separation [15]. Thus, biochar and magnetic biochar represents sustainable, low-cost, and effective alternatives to traditional treatment technologies, offering new hope for addressing the challenges of industrial wastewater, particularly from the textile sector [16]. Fig 1 shows the different biomass used to prepare biochar and magnetic biochar.

Fig: 1. Different biomass used to prepare biochar and magnetic biochar

2. Synthesis of Magnetic Biochar:

Biochar is a carbon-rich, porous solid produced through the pyrolysis of organic biomass under limited oxygen conditions [17]. This process thermally decomposes plant-based or organic materials, such as

agricultural residues, forestry waste, or aquatic plants like water hyacinth, to form a stable carbonaceous structure. The characteristics of the resulting biochar depend on factors like the type of biomass used, pyrolysis temperature, residence time, and heating rate [18]. For instance, low-temperature pyrolysis (300–500°C) retains more oxygenated functional groups and volatile matter, while high-temperature pyrolysis (above 600°C) yields biochar with higher carbon content, surface area, and porosity. These properties make biochar effective for pollutant adsorption, but unmodified biochar often exhibits limited affinity for specific contaminants such as dyes or heavy metals [19]. As a result, researchers have explored chemical and structural modifications to enhance its adsorptive performance, leading to the development of magnetic biochar. This magnetic functionality allows for the efficient removal and recycling of the adsorbent from aqueous solutions using an external magnetic field. There are two methods, named as co-precipitation technique and the impregnation-pyrolysis method which were using as iron precursors. Which may explain as follow.

2.1. Co-precipitation Technique

In the co-precipitation method is one of the most widely used and straightforward techniques for synthesizing magnetic biochar, primarily due to its simplicity, cost-effectiveness, and efficiency in producing uniformly dispersed magnetic nanoparticles. In this process, the biochar produced from pyrolysis is biochar immersed in an aqueous solution containing ferrous (Fe^{2+}) and ferric (Fe^{3+}) ions, commonly provided by ferrous chloride ($FeCl_2$) and ferric chloride ($FeCl_3$) in a 1:2 molar ratio, respectively [20].

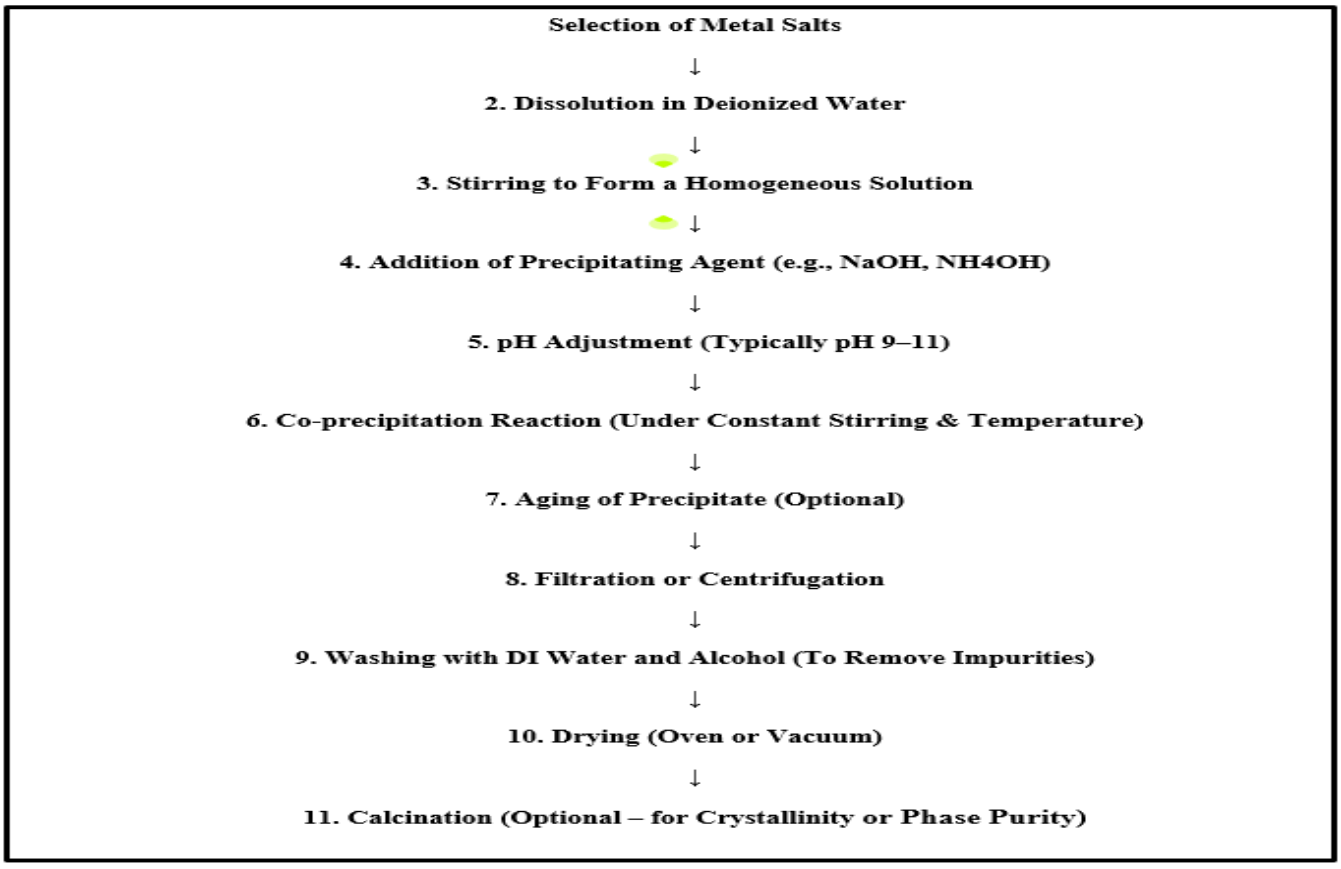

Fig: 2. Flow diagram to prepare Magnetic Biochar by Co-precipitation Technique

Once the biochar is well-treated with iron salt solution, and base such as sodium hydroxide (NaOH) or ammonium hydroxide (NH_4OH) is gradually added drop wise under constant stirring where the pH of the mixture is carefully adjusted to around 10, creating alkaline conditions that are essential for the simultaneous precipitation (co-precipitation) of iron ions. Under these conditions, the Fe^{2+} and Fe^{3+} ions react with hydroxide ions (OH^-) to form magnetite nanoparticles (Fe_3O_4) and produce porous structure of the biochar [21]. Fig. 2 shows the flow diagram to prepare Magnetic Biochar by Co-precipitation Technique. This step is typically followed by an aging process, where the suspension is allowed to stand or continue stirring for a designated period (e.g., several hours) at room temperature or mild heating to ensure complete precipitation and strong adhesion of Fe_3O_4 nanoparticles onto the biochar matrix [22]. The resulting magnetic biochar is then separated from the liquid phase through filtration or magnetic decantation, followed by repeated washing with deionized water or ethanol to remove unreacted chemicals, excess salts, and impurities. Finally, the washed material is dried at moderate temperatures (e.g., 60–80°C) to obtain the magnetic biochar composite. The magnetization of the biochar imparts a super paramagnetic or ferromagnetic character, allowing it to be easily separated from aqueous solutions using a simple external magnet [23]. This precipitated composite may use for adsorption of dyes, the detail Flow diagram to prepare Magnetic Biochar by Co-precipitation Technique may discuss as follow:

2.2. Impregnation and Pyrolysis with Iron Precursors:

In contrast to the co-precipitation method, the impregnation and pyrolysis technique involves introducing iron precursors into the raw biomass before the pyrolysis stage [24].

Fig:3. Flow diagram to prepare magnetic biochar by impregnation and pyrolysis with iron precursors

Here, the dried biomass is soaked in a solution of iron salts such as $FeCl_3$ or $Fe(NO_3)_3$, allowing the metal ions to penetrate the plant structure. After sufficient impregnation, the biomass is dried and then subjected to pyrolysis at elevated temperatures (typically 500–700°C). During the heating process, the iron salts thermally decompose into iron oxides like Fe_2O_3 or Fe_3O_4, which develop biochar matrix. This method ensures a strong bond between magnetic particles and the carbon structure, often resulting in more stable and efficient magnetic biochar for pollutant removal [25]. The magnetic biochar produced from either method particularly for the removal of dyes, heavy metals, and other industrial pollutants [26]. Fig. 3 shows the flow diagram to prepare magnetic biochar by impregnation and pyrolysis with iron precursors. Table 1 shows the comparison of Co-precipitation Technique and Impregnation and Pyrolysis with Iron Precursors method.

Table: 1. Comparison of Co-precipitation Technique and Impregnation and Pyrolysis with Iron Precursors method:

aspect	Co-precipitation Technique	Impregnation + Pyrolysis with Iron Precursors
Advantages		

Simple and low-cost synthesis	Easy to perform at low temperatures	Simple method for metal loading
Uniform particle distribution	Good control over nanoparticle size and distribution	Reasonable dispersion of iron on biomass
High magnetic properties	Effective in forming magnetic nanoparticles (e.g., Fe_3O_4) [27]	Magnetic properties retained after pyrolysis
Environmentally friendly	Aqueous medium, minimal toxic solvents	Biomass-based, sustainable approach
Fast reaction time	Co-precipitation Technique require short synthesis time [28]	Efficient in bulk production
Disadvantages		
pH-sensitive process	Requires precise pH control for precipitation	Not highly pH-sensitive, but process can affect material structure]
Particle agglomeration	Nanoparticles may cluster without surfactants or stabilizers [29]	Risk of metal sintering or uneven distribution during pyrolysis [31]
Low thermal stability	Not suitable for high-temperature applications	High temperatures may reduce surface area or porosity [32]
Complex post-processing	Requires washing, filtration, drying	Requires high-temperature furnace and inert gas environment
Limited loading capacity	Metal ion incorporation limited by solubility [30]	Iron loading depends on precursor soaking and biomass reactivity

2.4. Characterization Techniques of Magnetic Biochar:

There are some advanced techniques which are required to know the physico chemical structure of bioadsorbent, these characteristics evaluated the various properties like morphological structure of

bioadsorbent. Besides this some other properties like crystal structure and organic function group present in the material ‘may also determine [33].

2.4.1. Structural and Morphological Analysis (XRD, SEM):

X-ray diffraction (XRD) is important for identifying the crystalline phases present in magnetic biochar. It helps to know the crystal of magnetic iron oxides such as Fe_3O_4 or Fe_2O_3 into the carbon matrix. In the case of WH magnetic biochar, XRD patterns typically show distinct peaks around 30°, 35°, 43°, 57°, and 63° (2θ), corresponding to magnetite (Fe_3O_4) [34]. This confirms the magnetic modification. Scanning Electron Microscopy (SEM) provides insight the morphological structure reveals a rough, porous texture with well-distributed iron oxide particles across the surface. This porous structure is advantageous for dye and pollutant adsorption [35]. Table 2 shows the comparative Analysis of XRD and FTIR Spectra of Biochar and Magnetic Biochar.

Table .2: Comparative Analysis of XRD and FTIR Spectra of Biochar and Magnetic Biochar

Biomass Source	**Biochar Type / Treatment**	**XRD Observations**	**FTIR Observations (Major Functional Groups)**	**Ref.**
Rice Husk	Plain biochar (500°C)	Broad peak at 2θ ≈ 22–24° (amorphous carbon), sharp peaks at 26.6° (SiO_2 – quartz)	–OH (3400 cm^{-1}), Si–O–Si (1080 cm^{-1}), C–H (2920 cm^{-1}), C=C (1620 cm^{-1})	[36]
Rice Husk	Magnetic biochar ($FeCl_3$ impregnation + pyrolysis)	Fe_3O_4 peaks at 2θ ≈ 30.1°, 35.6°, 43.2°, 57.1°, 62.6°	Fe–O (580–590 cm^{-1}), Si–O–Si (1080 cm^{-1}), –OH (3430 cm^{-1}), C=O (1700 cm^{-1})	[37]
Water Hyacinth	Plain biochar	Broad hump at 2θ ≈ 23°, small peaks due to $CaCO_3$, SiO_2	–OH (3410 cm^{-1}), COOH (1710 cm^{-1}), C=C (1610 cm^{-1}), Si–O (1030 cm^{-1})	[38]
Water Hyacinth	Magnetic biochar ($FeSO_4$ + $FeCl_3$ co-precipitation)	Fe_3O_4 peaks + amorphous carbon, Ca-related phases	Fe–O (580 cm^{-1}), C–O–C (1120 cm^{-1}), –OH (3400 cm^{-1}), C=O (1710 cm^{-1})	[39]
Coconut Shell	Untreated biochar	Broad peak at ~24°, minor inorganic peaks	–OH (3430 cm^{-1}), aromatic C=C (1600 cm^{-1}), C–H (2910 cm^{-1}), C–O (1230 cm^{-1})	[40]

Coconut Shell	Magnetic biochar ($Fe(NO_3)_3$ impregnation)	Peaks of Fe_2O_3 at ~33.1°, 35.6°, 49.5°	Fe–O (around 570 cm^{-1}), –OH (3400 cm^{-1}), COOH (1705 cm^{-1})	[41]
Peanut Shell	Biochar at 500°C	Broad amorphous carbon hump, low crystallinity	–OH (3420 cm^{-1}), C=C (1590 cm^{-1}), C–O (1235 cm^{-1})	[42]
Peanut Shell	Magnetic biochar with Fe_3O_4	Characteristic Fe_3O_4 peaks, better crystallinity	Fe–O (575–590 cm^{-1}), –OH (3425 cm^{-1}), carboxylic C=O (1710 cm^{-1})	[43]
Corn Stover	$ZnCl_2$-activated biochar	Weak peak at 23°, ZnO or Zn-silicates	Zn–O (520 cm^{-1}), –OH (3400 cm^{-1}), C=O (1710 cm^{-1}), C–H (2915 cm^{-1})	[44]
Corn Stover	Magnetic biochar with iron salts	Magnetite (Fe_3O_4) peaks + Zn peaks	Fe–O (580 cm^{-1}), –OH, C=O, C–O observed	[45]
Sawdust	KOH-activated biochar	Broad amorphous carbon peaks, some K_2CO_3 or KCl	–OH (3435 cm^{-1}), C–O (1100 cm^{-1}), C=C (1600 cm^{-1}), C=O (1700 cm^{-1})	[46]
Sawdust	Magnetic biochar	Magnetite peaks (Fe_3O_4), suppressed K signals	Fe–O (580 cm^{-1}), –OH (3400 cm^{-1}), C–H (2910 cm^{-1}), aromatic groups	[47]

2.4.2. Surface Area and Porosity (BET):

The BET analysis is used know the specific surface area, pore size distribution, and pore volume of biochar [48]. These properties is directly related with adsorption potential of material. A higher surface area provides more active sites for pollutant binding. Magnetic biochar derived from WH often shows an increase in surface area compared to unmodified biochar due to the development of additional microspores during iron incorporation [49].

2.4.3. Functional Groups and Surface Chemistry (FTIR):

(FTIR) is used to know the functional groups present on the surface of the biochar. These functional groups—such as hydroxyl (-OH), carboxyl (-COOH), and carbonyl (C=O)—play a key role in adsorption through mechanisms like hydrogen bonding and electrostatic interaction For WH magnetic

biochar, FTIR spectra often show peaks related to O–H stretching, C–H bending, and Fe–O vibrations, representing the successful loading of iron oxides and the retention of oxygen-containing groups that contribute to effective dye or heavy metal removal [50].

2.4.4. Magnetic Properties (VSM): VSM analysis is directed to know the magnetic properties of the synthesized biochar, particularly to know its suitability for applications involving magnetic separation. VSM is a powerful technique that determine key magnetic parameters such as saturation magnetization (Ms), coercivity (Hc), and remanent magnetization (Mr). These parameters afford strength of the magnetic response of the material. Magnetic biochar often demonstrates super paramagnetic behaviour, which is desirable for environmental remediation [51]. The typical saturation magnetization values for WH-based magnetic biochar range between 10–30 emu/g, which are sufficient for fast and efficient magnetic recovery from aqueous systems. This magnetic recoverability eliminates the need for time-consuming and costly separation methods such as filtration or centrifugation. As a result, magnetic biochar can be easily reused, making it an economical and sustainable solution for wastewater treatment applications [52]. Table3 shows the comparative analysis of magnetic vs. non-magnetic biochar in wastewater treatment.

Table.3: Comparative analysis of magnetic vs. non-magnetic biochar in wastewater treatment

S.No.	Biomass Source	Pollutant	Non-Magnetic Biochar Removal Efficiency (%)	Magnetic Biochar Removal Efficiency (%)	Advantages of Magnetic Biochar	Disadvantages of Magnetic Biochar	References.
1	Rice Husk	Crystal Violet	~50%	>90%	Enhanced adsorption capacity	Potential for secondary pollution if not properly managed	[53]
2	Coconut Shell	Acid Orange	~60%	>95%	Improved removal efficiency	Increased production cost	[54]
3	Chicken Bones	Rhoda mine B	~45%	75%	Better adsorption kinetics	Possible leaching of iron	[55]

4	Wheat Straw	Methylene Blue	~70%	>90%	Faster equilibrium time	Reduced surface area due to magnetization	[56]
5	Sewage Sludge	Methylene Blue	~54%	~56%	Slight improvement in removal	Marginal benefits over non-magnetic biochar	[57]
6	Partheni umstero phorus	Methylene Blue	94%	99.99%	Significant enhancement in efficiency	Complex synthesis process	[58]
7	Rice Bran	Ni(II)	~60%	>90%	Higher adsorption capacity	Potential environmenta l risks	[59]
8	Bagasse	Cr(VI)	~50%	>85%	Improved heavy metal removal	Possible iron leaching	[60]
9	Corn Stalk	Pb(II)	~65%	>90%	Enhanced adsorption sites	Higher synthesis cost	[61]
10	Water Hyacinth	Methylene Blue	~70%	>95%	Better pollutant removal	Potential for nanoparticle release	[62]
11	Peanut Shell	Cr(VI)	~55%	>80%	Improved adsorption efficiency	Increased production complexity	[63]
12	Bamboo	Methylene Blue	~60%	>90%	Faster adsorption rates	Potential environmenta l concerns	[64]
13	Sugarcan e Bagasse	Pb(II)	~70%	>95%	Higher removal efficiency	Possible secondary pollution	[65]

14	Corn Cob	Ni(II)	~60%	>85%	Enhanced adsorption capacity	Increased synthesis cost	[66]
15	Sawdust	Cd(II)	~50%	>80%	Improved heavy metal removal	Potential for iron leaching	[67]
16	Algal Biomass	Methylene Blue	~65%	>90%	Better dye removal	Complex preparation process	[68]
17	Fruit Peels	Cr(VI)	~55%	>85%	Enhanced adsorption sites	Higher production cost	[69]
18	Wood Chips	Pb(II)	~60%	>90%	Improved heavy metal removal	Potential environmental risks	[70]
19	Rice Straw	Methylene Blue	~70%	>95%	Higher removal efficiency	Possible nanoparticle release	[71]
20	Orange Peel	Cd(II)	~50%	>80%	Enhanced adsorption capacity	Increased synthesis complexity	[72]

3. Properties and Applications of Magnetic Biochar in Wastewater Treatment.

3.1. Adsorption Capabilities:

Magnetic biochar is a planned material created by integrating magnetic nanoparticles—commonly iron oxides such as Fe_3O_4 or γ-Fe_2O_3—into traditional biochar derived from biomass sources like agricultural waste [73]. This modification conveys the resulting composite with unique physicochemical and magnetic properties, significantly improving its adsorption capabilities and ease of separation in wastewater treatment applications. One of the most important advantages of magnetic biochar lies in its physicochemical properties, which make it highly effective in removing dyes and heavy metals from contaminated water [74]. Its high surface area provides a larger number of active sites for adsorption, while its porous structure—particularly the presence of micro- and mesopores—facilitates the diffusion

and trapping of pollutants like dye molecules and metal ions. Furthermore, magnetic biochar surfaces often contain abundant oxygen-containing functional groups such as hydroxyl (–OH), carboxyl (–COOH), and amino ($–NH_2$) groups, which actively interact with pollutants through mechanisms like hydrogen bonding, electrostatic interactions, and surface complexion [75]. The pH-responsive nature of these functional groups plays a key role in adsorption efficiency, especially for metal ions, as it affects ionization states and binding affinities.

3.2. Essential magnetic property:

Another distinctive feature of magnetic biochar is its inherent magnetic property, which allows for easy recovery after treatment. This feature provides a significant operational benefit in post-treatment processes. After adsorption, the magnetic biochar can be separated from the treated water using an external magnet [76]. This eliminates the need for multifaceted filtration or centrifugation systems, reduces processing time, and minimizes operational costs. More importantly, it reduces the risk of secondary pollution caused by the loss of fine biochar particles in the effluent stream. Such ease of separation is particularly advantageous in continuous treatment systems or large-scale operations, where time and material recovery are important parameters [77].

3.3. Performance of dyes and heavy metal removal:

In textile water treatment it is found that the performance to remove heavy metal and dye removal is good if the solution is treated by magnetic biochar. It is investigated that magnetic biochar has excellent performance in removing cationic dyes like methylene blue (MB) and anionic dyes like Congo red (CR). These dyes are adsorbed through various mechanisms including π–π interactions, electrostatic attractions, and pore-filling effects [78]. The Removal efficiencies for methylene blue using magnetic biochar frequently exceed 90–95% under optimal conditions, while Congo red, owing to its anionic nature, is efficiently captured via electrostatic attraction to positively charged functional groups on the biochar surface. In the case of heavy metals such as hexavalent chromium (Cr^{6+}), lead (Pb^{2+}), and copper (Cu^{2+}), magnetic biochar shows strong adsorption through ion exchange, and electrostatic interactions[68] Several studies have reported Cr^{6+} removal efficiencies close to 98–99%, while Pb^{2+} and Cu^{2+} are also effectively removed by interacting carboxyl COOH- and hydroxyl groups OH- group present on the magnetic biochar matrix[79] .In addition to its high adsorption efficiency, magnetic biochar has excellent regeneration and reusability potential. The Spent magnetic biochar can be regenerated through desorption methods using mild acid, base, or salt solutions, and in some cases, by thermal reactivation. These regeneration methods can restore the adsorption capacity, allowing the biochar to be reused multiple times. Studies have shown that magnetic biochar retains over 80–90% of its original adsorption performance

even after four to five cycles of use [80]. This not only reduces the overall cost of treatment but also contributes to the development of an environmentally friendly and circular water treatment system.

4. Adsorption Isotherm and Kinetic Modelling:

It is important to understand to validate the adsorption and kinetic models is fundamental to estimating the efficiency, mechanism, and feasibility of adsorbents in wastewater treatment applications [81]. The Adsorption isotherms express that how pollutants interact with the surface of the adsorbent at equilibrium it also helps to quantify the adsorption capacity. Table 4 shows the comparative Table: Biochar Performance Based on Pollutant Type.

Table 4: Comparative Table: Biochar Performance Based on Pollutant Type

Biochar Source	Activation/Modification	Target Pollutants	Pollutant Type	Adsorption Behaviour/ Performance	Ref.
Rice Husk	H_3PO_4 activation	Methylene Blue (MB), Pb^{2+}	Cationic dye, Heavy metal	High surface area; electrostatic attraction and pore diffusion	[82]
Water Hyacinth	Magnetic biochar (Fe_3O_4)	Congo Red (CR), Cr(VI)	Anionic dye, Metal ion	Good removal via electrostatic binding and redox with Fe^{3+}/Fe^{2+}	[83]
Coconut Shell	$ZnCl_2$ activation	Rhodamine B, Cu^{2+}	Cationic dye, Metal	$ZnCl_2$ improves microporosity; adsorption via surface complexation	[84]
Corn Stover	Fe-impregnated biochar	Arsenic (As(V)), Nitrate	Metalloid, Anion	Fe provides reactive sites for ligand exchange and reduction	[85]
Banana Peel	Untreated / base-treated	Pb^{2+}, Cd^{2+}	Heavy metals	Surface functional groups (–OH, –COOH) aid metal ion complexation	[86]

Peanut Shell	Magnetic (Fe_3O_4-coated)	Methylene Blue, Cr(VI)	Dye, Metal ion	Magnetic separation + high surface binding; Fe_3O_4 aids reduction	[87]
Wheat Straw	KOH activation	Reactive Black 5	Anionic dye	High surface area and π–π interactions with aromatic rings	[88]
Sugarcane Bagasse	Acid treatment	Tannic acid, Zn^{2+}	Organic acid, Metal ion	Carboxylic groups bind metals and organics; low-cost sorbent	[89]
Sawdust	NaOH activation	Phenol, Ni^{2+}	Organic, Metal ion	Surface oxygen functional groups enhance binding	[90]
Pine Wood	Magnetic with Fe/Co oxides	Cr(VI), Methylene Blue	Metal, Dye	Dual redox-adsorption pathways; good recyclability	[91]

4.1. Adsorption Isotherm: On the hand the adsorption kinetic models, which define the rate at which adsorption occurs and provide information about the rate-controlling steps It is important to understand adsorption isotherm and kinetic models to know feasibility of adsorbents in wastewater treatment and how pollutants interact with the surface of the adsorbent at equilibrium, helping to count the adsorption capacity [92]. Among the most widely used isotherms is the Langmuir model, which assumes monolayer adsorption onto a homogeneous surface with finite identical sites. This model is particularly useful for predicting maximum adsorption capacities and helps in designing adsorption systems for industrial applications.

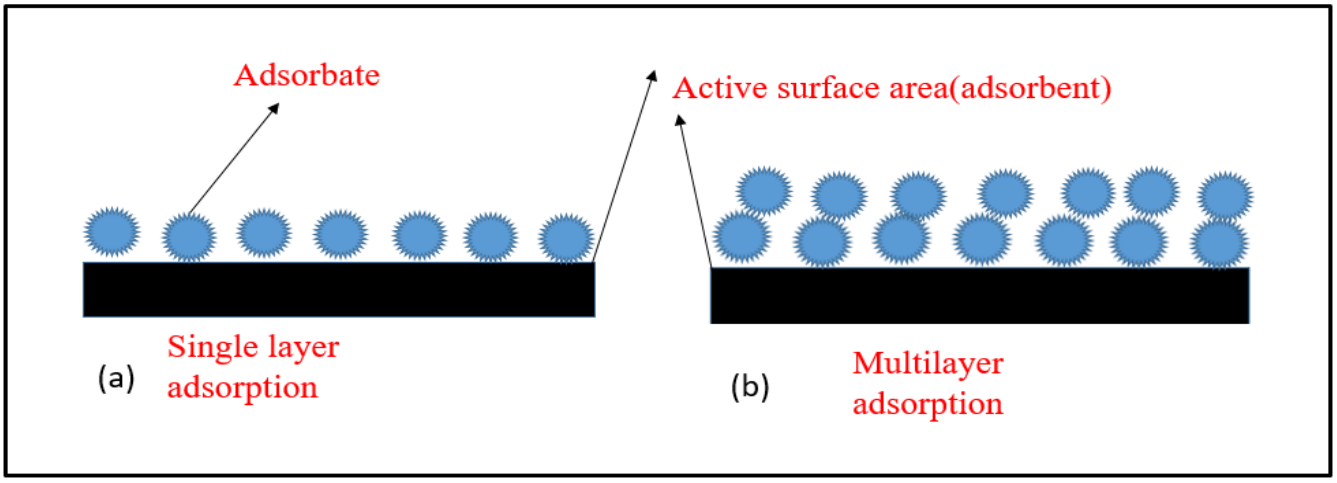

Fig. 4 (a) Single layer adsorption (b) Multilayer adsorption process

While with the help of the Freundlich isotherm accounts for multilayer adsorption on a heterogeneous surface and is better suited for describing adsorption in real and complex systems such as textile wastewater containing multiple pollutants [93]. Fig. 4 (a) shows single layer adsorption and 4 (b) Multilayer adsorption process. Additionally, the Temkin isotherm considers the effect of indirect adsorbate/adsorbent interactions, while the Dubinin–Radushkevich (D–R) model helps to distinguish between physical and chemical adsorption processes based on the mean free energy of adsorption. These all models provide comprehension into adsorption mechanisms—whether driven by ion exchange, pore filling, or chemical bonding—and supports optimization of operational parameters [94]

4.2. Adsorption kinetics:

The pseudo-first-order kinetic model is often used for systems where physical adsorption dominates, as it assumes that the rate of occupation of adsorption sites is proportional to the number of unoccupied sites. However, many studies find the pseudo-second-order model better describes the kinetics of biochar and magnetic biochar systems, indicating chemisorption as the primary mechanism involving electron sharing or exchange between adsorbent and adsorbate [95]. The applicability of these kinetic models is typically assessed through correlation coefficients and error analysis. To further probe into the adsorption mechanism, models like the intra-particle diffusion model are used to determine whether diffusion through pores or boundary layers is the rate-limiting step. Similarly, the Elovich model is helpful for systems with heterogeneous surfaces and where adsorption activation energy varies during the process [96]. Together, these isotherm and kinetic models offer a comprehensive understanding of how pollutants like dyes or heavy metals are removed from wastewater using magnetic or non-magnetic biochar. They guide the scaling-up of laboratory findings to real-world applications by predicting performance under various conditions. More importantly, validating these models helps researchers and engineers in optimizing adsorbent dosage, contact time, pH, and temperature to achieve cost-effective and sustainable water purification solutions. Hence,

incorporating and verifying both isotherm and kinetic modelling is not only scientifically significant but also crucial for advancing practical applications in environmental remediation [97]. Table 5 shows the comparison review of removal efficiency of biochar and their magnetic biochar prepared from various biomass.

Table.5: Comparison review of removal efficiency of biochar and their magnetic biochar prepared from various biomass

S no.	Biomass Source	Pollutant	Isotherm Models	Kinetic Models	Non-Magnetic Biochar Removal Efficiency (%)	Magnetic Biochar Removal Efficiency (%)	Parameters	Ref.
2	Coconut Shell	Acid Orange	Langmuir	Pseudo-Second-Order	~60%	>95%	pH 3, 30°C, 1 g/100 ml, 90 min contact time	[98]
3	Chicken Bones	Rhodamine B	Langmuir, Freundlich	Pseudo-First-Order	~45%	75%	pH 7, 25°C, 0.3 g/50 ml, 60 min contact time	[99]
4	Wheat Straw	Methylene Blue	Langmuir, Temkin	Pseudo-Second-Order	~70%	>90%	pH 8, 35°C, 0.5 g/100 ml, 120 min contact time	[100]
5	Sewage Sludge	Methylene Blue	Freundlich	Elovich	~54%	~56%	pH 6, 25°C, 1 g/100 ml, 90 min contact time	[101]
6	Partheni um hysteron phorus	Methylene Blue	Langmuir, Freundlich	Pseudo-Second-Order	94%	99.99%	pH 9, 30°C, 0.2 g/50 ml, 60 min contact time	[102]

7	Rice Bran	Ni(II)	Langmuir	Pseudo-Second-Order	~60%	>90%	pH 6, 40°C, 1 g/100 ml, 120 min contact time	[103]
8	Bagasse	Cr(VI)	Langmuir, Temkin	Pseudo-Second-Order	~50%	>85%	pH 2, 25°C, 1 g/100 ml, 90 min contact time	[104]
9	Corn Stalk	Pb(II)	Langmuir, Freundlich	Intra-Particle Diffusion	~65%	>90%	pH 5, 25°C, 0.5 g/100 ml, 60 min contact time	[105]
10	Water Hyacinth	Methylene Blue	Langmuir, Freundlich	Pseudo-Second-Order	~70%	>95%	pH 7, 30–50°C, 20–30 mg/25 ml, 60–90 min contact time	[106]
11	Peanut Shell	Cr(VI)	Langmuir, Dubinin-Radushkevich	Elovich	~55%	>80%	pH 2, 40°C, 1 g/100 ml, 120 min contact time	[107]
12	Bamboo	Methylene Blue	Langmuir	Pseudo-Second-Order	~60%	>90%	pH 7, 30°C, 0.2 g/50 ml, 60 min contact time	[108]
13	Sugarcane Bagasse	Pb(II)	Langmuir, Freundlich	Pseudo-First-Order	~70%	>95%	pH 6, 25°C, 0.5 g/100 ml, 90 min contact time	[109]
14	Corn Cob	Ni(II)	Freundlich	Pseudo-Second-Order	~60%	>85%	pH 5.5, 40°C, 0.4 g/100 ml, 90	[110]

							min contact time	
15	Sawdust	Cd(II)	Langmuir, Temkin	Pseudo-Second-Order	~50%	>80%	pH 5.5, 30°C, 1 g/100 ml, 60 min contact time	[111]
16	Algal Biomass	Methylene Blue	Langmuir, Freundlich	Intra-Particle Diffusion	~65%	>90%	pH 8, 25°C, 0.3 g/50 ml, 90 min contact time	[112]
17	Fruit Peels	Cr(VI)	Freundlich	Pseudo-Second-Order	~55%	>85%	pH 2, 35°C, 0.5 g/100 ml, 120 min contact time	[113]
18	Wood Chips	Pb(II)	Langmuir	Pseudo-Second-Order	~60%	>90%	Flow rate 5 ml/min, bed height 5 cm, pH 5	[114]
19	Rice Straw	Methylene Blue	Langmuir, Freundlich	Pseudo-Second-Order	~70%	>95%	pH 7, 30°C, 0.5 g/100 ml, 60–90 min contact time	[115]
20	Orange Peel	Cd(II)	Temkin, Freundlich	Elovich	~50%	>80%	pH 6, 25°C, 1 g/100 ml, 60 min contact time	[116]

The Comparison of magnetic and non-magnetic bio chars derived from various biomass sources reveals a significant enhancement in pollutant removal efficiency upon magnetization. Rice husk biochar exhibited an increase in Crystal Violet removal from ~50% to over 90% under pH 6, 40°C, with 0.5 g/100 ml dosage and 60 minutes of contact time [98]. Similarly, coconut shell biochar showed improved Acid Orange removal from ~60% to >95% at pH 3, 30°C, and 1 g/100 ml dosage over 90 minutes [99]. Chicken bone-based biochar

improved Rhoda mine B adsorption efficiency from ~45% to 75% under pH 7, 25°C, 0.3 g/50 ml, in 60 minutes [44]. Wheat straw demonstrated a jump in Methylene Blue removal from ~70% to >90% at pH 8, 35°C, and 0.5 g/100 ml in 120 minutes [100]. Notably, sewage sludge biochar showed minimal improvement in Methylene Blue adsorption, rising only slightly from ~54% to ~56%, under pH 6, 25°C, 1 g/100 ml for 90 minutes [101]. Ruthenium hysterophorus-derived biochar displayed high efficiency, increasing Methylene Blue removal from 94% to nearly complete at 99.99%, with optimal parameters of pH 9, 30°C, and 0.2 g/50 ml in 60 minutes [102]. Rice bran-based bio char's Ni(II) removal rose from ~60% to >90% at pH 6, 40°C, and 1 g/100 ml in 120 minutes [103], while bagasse showed a significant improvement in Cr(VI) removal from ~50% to >85% at pH 2, 25°C, and 1 g/100 ml for 90 minutes [104]. Corn stalk biochar increased Pb(II) removal from ~65% to >90% under pH 5, 25°C, 0.5 g/100 ml, and 60 minutes [105]. Water hyacinth biochar showed a substantial improvement in Methylene Blue removal from ~70% to >95% at pH 7, 30–50°C, with 20–30 mg in 25 ml solution for 60–90 minutes [106]. For Cr(VI), peanut shell-based biochar improved from ~55% to >80% under pH 2, 40°C, 1 g/100 ml, and 120 minutes [107], while bamboo-based biochar increased Methylene Blue removal from ~60% to >90% at pH 7, 30°C, and 0.2 g/50 ml in 60 minutes [108]. Sugarcane bagasse improved Pb (II) removal from ~70% to >95% at pH 6, 25°C, with 0.5 g/100 ml in 90 minutes [109]. Corn cob enhanced Ni(II) removal from ~60% to >85% at pH 5.5, 40°C, and 0.4 g/100 ml in 90 minutes [110], and sawdust-based biochar increased Cd(II) adsorption from ~50% to >80% under pH 5.5, 30°C, 1 g/100 ml, and 60 minutes [111].Algal biomass biochar improved Methylene Blue removal from ~65% to >90% at pH 8, 25°C, and 0.3 g/50 ml in 90 minutes [112], while fruit peel biochar enhanced Cr(VI) removal from ~55% to >85% at pH 2, 35°C, and 0.5 g/100 ml in 120 minutes [113]. Wood chip biochar showed a rise in Pb (II) removal from ~60% to >90%, under continuous flow at 5 ml/min, 5 cm bed height, and pH 5 [114]. Rice straw-based biochar increased Methylene Blue removal from ~70% to >95% at pH 7, 30°C, 0.5 g/100 ml, and 60–90 minutes of contact [115]. Lastly, orange peel biochar enhanced Cd II) removal from ~50% to >80% at pH 6, 25°C, 1 g/100 ml, and 60 minutes [116].

5. Mechanisms of Pollutant Removal Using Magnetic Biochar

This permits the pollutants to be physically trapped within the micro pores and mesopores—a process referred to as pore filling. At the same time, surface complexion occurs when metal ions form coordination bonds with surface functional groups like –COOH and –OH [117]. These interactions are often stronger and more specific than physical adsorption and become reason to be chemisorption [118]. Evidence of complexion can be observed through techniques like FTIR, which reveal shifts in characteristic functional group peaks following adsorption. Another important class of interactions includes π–π interactions and hydrogen bonding [119], especially relevant in the adsorption of organic pollutants with aromatic structures. The π–π interactions take place between the aromatic rings present in dye molecules and the conjugated aromatic systems in lignin

or carbonized biomass surfaces [120]. Hydrogen bonding, on the other hand, involves interactions between polar functional groups on the pollutant and the biomass, particularly –OH, –NH_2, and –COOH groups [121]. These interactions not only enhance adsorption capacity but also contribute to the stability of the adsorbed species on the biomass surface [122]. Fig. 5 shows the mechanisms of pollutant removal using magnetic biochar.

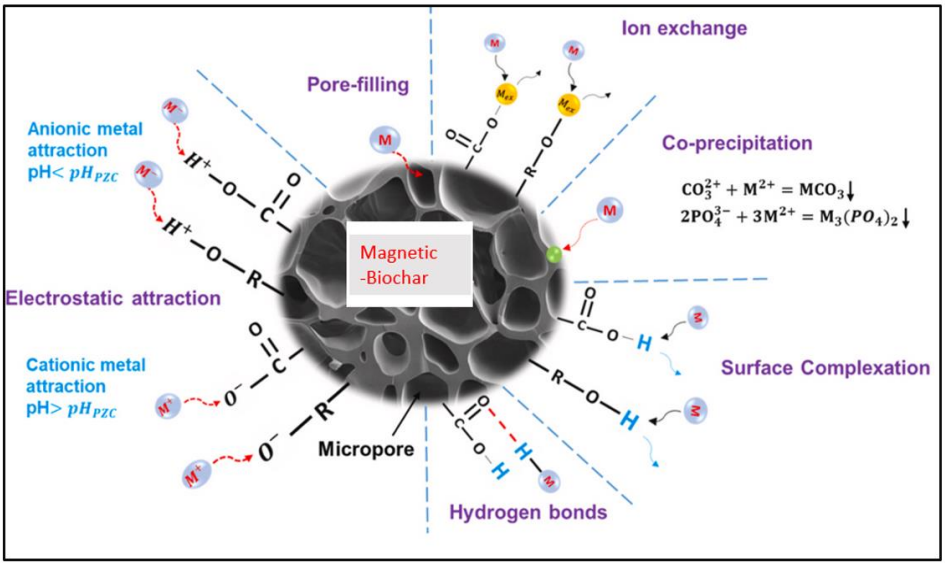

Fig .5: Mechanisms of pollutant removal using magnetic biochar (adopted from [122])

5.1. Fenton-Like Catalytic Degradation Potential

Beyond passive adsorption, certain biomass-derived materials exhibit Fenton-like catalytic degradation properties, especially after thermal or chemical treatment. These materials may retain residual transition metals like iron (Fe), copper (Cu), or manganese (Mn), which can activate hydrogen peroxide (H_2O_2) to produce highly reactive hydroxyl radicals (•OH). This oxidative process results in the degradation of complex organic pollutants [123]. The classical Fenton reaction involves Fe^{2+} reacting with H_2O_2 to generate •OH radicals, which then oxidize dye molecules or other contaminants into smaller, less harmful products. Such reactions provide a dual mechanism of pollutant removal—adsorption followed by chemical degradation—which enhances the overall efficiency [124]. For instance, calcined water hyacinth ash, known to retain iron content, has demonstrated Fenton-like activity, making it effective in the degradation of Methylene Blue dye beyond what can be achieved by adsorption alone. Table 6 shows the linkage between pollutant removal mechanism and appropriate adsorption kinetics.

Table .6: Linkage between Pollutant Removal Mechanism and Appropriate Adsorption Kinetics

Pollutant	**Removal Mechanism**	**Best-Fit Kinetic Model**	**Why This Model is Appropriate**	**Ref.**
Methylene Blue (MB) (Cationic dye)	Electrostatic attraction to negatively charged sites; pore diffusion; π–π stacking	Pseudo-second-order	Chemisorption dominates via electron sharing/exchange between dye and surface functional groups	[125]
Congo Red (CR) (Anionic dye)	Electrostatic interaction with positively charged surface; H-bonding	Pseudo-second-order	Involves valence forces or surface complexation, indicating chemisorption	[126]
Reactive Black 5 (Anionic dye)	Electrostatic bonding and π–π interactions	Pseudo-second-order	Rate controlled by surface interactions, not just dye concentration	[127]
Pb^{2+} (Lead ion)	Surface complexation with –COOH/–OH; ion exchange	Pseudo-second-order	Strong interaction and possible chemical bonding with surface ligands	[128]
Cd^{2+} (Cadmium ion)	Ion exchange, surface complexation	Pseudo-second-order	Chemisorption likely due to inner-sphere complexation on active sites	[129]
Cu^{2+} (Copper ion)	Ion exchange; precipitation on surface; coordination with O/N groups	Pseudo-second-order	Involves coordination-type adsorption — slower and more chemically controlled	[130]
Ni^{2+} (Nickel ion)	Complexation with surface oxygen functional groups	Pseudo-second-order	Adsorption governed by rate-limiting chemisorption step	[131]
Cr(VI)	Electrostatic attraction; redox reaction (Cr(VI) → Cr(III))	Pseudo-second-order	Adsorption + redox (chemical transformation), fitting second-order assumptions	[132]

5.2. Synergistic Effects of Iron Nanoparticles in Pollutant Removal:

The incorporation of iron nanoparticles (Fe_3O_4) into biomass-based adsorbents introduces powerful synergistic effects in pollutant removal. These composites not only exhibit enhanced adsorption but also enable magnetic separation, facilitating easy recovery and reuse [133]. Iron nanoparticles contribute to pollutant degradation through several pathways, including reductive transformation, where zero-valent iron (Fe^0) reduces contaminants like Cr (VI) to less toxic forms such as Cr (III). Additionally, in the presence of H_2O_2, Fe-based nanocomposites can catalyse Fenton-like reactions, as previously discussed, further breaking down dyes, pharmaceuticals, and pesticides [134]. The synergistic effects stem from the combination of high surface area, active metal sites, and reactive oxygen species generation. These features make Fe-loaded biomass materials, such as Fe–biochar or Fe–modified water hyacinth adsorbents, highly effective and versatile platforms for treating a wide range of water pollutants [135].

5.3. The Reusability of the biochar material:

The reuse performance of biochar as an adsorbent is influenced by several critical factors. One primary issue is the saturation of active sites**,** where adsorption sites become occupied by pollutants, reducing the bio char's capacity in subsequent cycles [136]. Additionally, structural degradation can occur during repeated washing or regeneration processes—especially under high-temperature treatments or chemical exposure—which may lead to the breakdown of the bio char's porous structure. Another key factor is the loss of surface functional groups such as –OH and –COOH, which play a crucial role in pollutant binding; these groups can be stripped away during acid or base regeneration, resulting in diminished adsorption efficiency [137]. Furthermore**,** incomplete desorption of previously adsorbed pollutants can block microspores or active sites, limiting the material's effectiveness in later cycles. For magnetic biochar**,** especially those based on iron (Fe), corrosion or leaching of iron may occur, leading to reduced magnetic recovery efficiency and a decline in reactive surface functionality. In terms of observable trends across reuse cycles, a noticeable decline in performance is often recorded. Between the first and second reuse cycles, an efficiency loss of about 5–15% is commonly observed [138]. This loss can increase to 10–25% by the third cycle. If regeneration is not properly optimized, biochar may experience up to 40% efficiency reduction after five cycles. These performance losses highlight the importance of understanding and mitigating the degradation mechanisms associated with biochar reuse.

5.4. Method or approach to demonstrate the reusability of the biochar material:

To evaluate and demonstrate the reusability of biochar, several methods can be employed. Batch desorption–adsorption studies involve measuring the recovery of adsorption capacity by desorbing pollutants with mild agents (e.g., acid, base, or ethanol) after each cycle and reintroducing the pollutant to assess performance. Thermal regeneration tests assess the structural stability of biochar by heating it at 300–500°C

under an inert atmosphere and monitoring changes in surface area. Characterization techniques such as FTIR, XRD, and SEM are used before and after reuse cycles to evaluate alterations in functional groups, surface morphology, and crystallinity [139]. For magnetic biochar**,** magnetic recovery tests help determine separation efficiency and magnetic strength across cycles. Additionally, leaching tests are conducted to ensure environmental safety by checking for metal ion release (e.g., Fe, Zn) from spent biochar. A standard approach to test reusability includes running at least five adsorption–desorption cycles using a fixed biochar dose (e.g., 20 mg/25 mL) and known pollutant concentration under controlled pH and temperature conditions. Regeneration is performed using a mild desorbing agent such as 0.1 M HCl for metals or 0.1 M NaOH for dyes. Performance is evaluated through removal efficiency, desorption efficiency, and mass loss per cycle**.** After the final cycle, comparative characterization (BET, FTIR, SEM–EDS) is used to assess structural and chemical changes [140]. For example, adsorption efficiency may decrease from 92% in the first cycle to around 74% by the fifth, with corresponding decreases in desorption efficiency and remaining capacity. This protocol provides a comprehensive and practical framework to demonstrate the reusability and long-term efficiency of biochar-based adsorbents.

6. Future Perspectives:

Despite significant progress in utilizing biomass-derived adsorbents, particularly water hyacinth-based materials, several research gaps and limitations remain. Most studies to date have focused on batch experiments under controlled laboratory conditions, often with synthetic dye solutions [141]. These do not always represent the complex matrices found in real industrial effluents. Furthermore, there is a lack of understanding regarding the long-term stability, desorption behaviour, and regeneration capacity of these adsorbents over multiple cycles. Limited insights into the exact mechanistic pathways, particularly under variable environmental conditions such as fluctuating pH, ionic strength, and competing ions, also constrain the comprehensive application of these materials [142]. Additionally, in-depth toxicological studies on the release of any potentially harmful by-products or residual materials after treatment are still underexplored. One of the most pressing concerns is the scale-up and industrial feasibility of using water hyacinth-based or magnetic biochar materials. While lab-scale results are promising, scaling the production process to an industrial level introduces challenges such as consistent raw material supply, cost-effectiveness of activation or nanoparticle loading processes, and the management of secondary waste streams [143]. The variability in biomass composition due to geographic, seasonal, or environmental differences may also affect reproducibility and adsorbent performance on a commercial scale. Moreover, integration into existing wastewater treatment systems requires standardized operating parameters and compliance with regulatory frameworks, which are yet to be fully addressed. In terms of future directions, there is growing interest in developing magnetic biochar composites with enhanced functionalities [144]. These materials offer promising Advantages such as easy

separation using external magnetic fields, improved reusability, and dual-functionality for both adsorption and catalytic degradation. Future research could focus on green synthesis techniques for embedding iron or other transition metal nanoparticles into biochar matrices, reducing the reliance on harsh chemicals and minimizing environmental impact. Advanced characterization methods like synchrotron-based spectroscopy, electron tomography, and real-time in situ monitoring can help unravel the dynamic interactions between pollutants and biochar surfaces [145]. Additionally, exploring synergistic combinations with photo catalytic or microbial systems may lead to the next generation of hybrid pollutant removal technologies.

7. Conclusion:

Water hyacinth-based bioadsorbent, especially when modified into magnetic nanocomposites, represent a sustainable and low-cost approach to tackle water pollution. Their multifaceted adsorption mechanisms, coupled with catalytic and magnetic properties, make them suitable candidates for real-world applications. However, to fully realize their potential, future research must address scale-up challenges, ensure environmental safety, and optimize performance under practical conditions. Continued interdisciplinary collaboration among material scientists, environmental engineers, and industrial stakeholders will be essential to translate laboratory innovations into field-ready solutions for sustainable wastewater treatment.

List of Abbreviations

BOD – Biological Oxygen Demand
COD – Chemical Oxygen Demand
MB – Methylene Blue
CR – Congo Red
XRD – X-ray Diffraction
SEM – Scanning Electron Microscopy
BET – Brunauer–Emmett–Teller (surface area analysis)
FTIR – Fourier Transform Infrared Spectroscopy
VSM – Vibrating Sample Magnetometry

Author Contributions

Conceptualization, methodology, software: **DBP, AK**.; Validation, formal analysis, funding acquisition: **AK.**; Investigation, resources, data curation, writing—original draft preparation, writing—review and editing, visualization, supervision, project administration: **GLD, AKR, AK and DBP.** All authors have read and agreed to the published version of the manuscript.

Conflicts of Interest

The authors declare that there is no conflict of interest regarding the publication of this article.

Funding

Not applicable.

Acknowledgement

The authors AK, AK, GLD and DBP thankful to HBTU Kanpur Uttar Pradesh, India for necessary facilities.

References:

[1] Smail, E.A., DiGiacomo, P.M., Seeyave, S., Djavidnia, S., Celliers, L., Le Traon, P.Y., Gault, J., Escobar-Briones, E., Plag, H.P., Pequignet, C. and Bajona, L., 2019. An introduction to the 'Oceans and Society: Blue Planet'initiative. *Journal of Operational Oceanography*, *12*(sup2), pp.S1-S11-

[2] Mishra, R.K., 2023. Fresh water availability and its global challenge. *British Journal of Multidisciplinary and Advanced Studies*, *4*(3), pp.1-78.

[3] Shafik, W., 2025. Pathways to Climate Neutrality: Understanding Ice Cap Reduction, Glacial Melt, and Sea Level Change and Adoption. In *Climate Neutrality Through Smart Eco-Innovation and Environmental Sustainability* (pp. 53-67). Cham: Springer Nature Switzerland.

[4] Thorson, N.W., 1978. Storing water underground: What's the aqui-fer. *Neb. L. Rev.*, *57*, p.581

[5] Pradinaud, C., Northey, S., Amor, B., Bare, J., Benini, L., Berger, M., Boulay, A.M., Junqua, G., Lathuillière, M.J., Margni, M. and Motoshita, M., 2019. Defining freshwater as a natural resource: a framework linking water use to the area of protection natural resources. *The international journal of life cycle assessment*, *24*, pp.960-974

[6] Duda, A.M., 1993. Addressing nonpoint sources of water pollution must become an international priority. *Water Science and Technology*, *28*(3-5), pp.1-11

[7] Kumar, P.S. and Saravanan, A., 2017. Sustainable wastewater treatments in textile sector. In *Sustainable fibres and textiles* (pp. 323-346). Woodhead Publishing.

[8] Daud, M.K., Nafees, M., Ali, S., Rizwan, M., Bajwa, R.A., Shakoor, M.B., Arshad, M.U., Chatha, S.A.S., Deeba, F., Murad, W. and Malook, I., 2017. Drinking water quality status and contamination in Pakistan. *BioMed research international*, *2017*(1), p.7908183.

[9] Sall, M.L., Diaw, A.K.D., Gningue-Sall, D., Efremova Aaron, S. and Aaron, J.J., 2020. Toxic heavy metals: impact on the environment and human health, and treatment with conducting organic polymers, a review. *Environmental Science and Pollution Research*, *27*, pp.29927-29942.

[10] Thomas, C.T., 2021. *Photocatalytic treatment of biological organisms in water using graphene oxide doped TiO2 and BiVO4 nanocomposites* (Doctoral dissertation, Le Mans Université; Centro de Investigación y de Estudios Avanzados del Instituto Politécnico Nacional (Mexico)).

[11] Sapari, N., 1996. Treatment and reuse of textile wastewater by overland flow. *Desalination*, *106*(1-3), pp.179-182.

[12] Ersahin, M.E., Ozgun, H., Dereli, R.K., Ozturk, I., Roest, K. and van Lier, J.B., 2012. A review on dynamic membrane filtration: materials, applications and future perspectives. *Bioresource technology*, *122*, pp.196-206.

[13] Deng, Y. and Zhao, R., 2015. Advanced oxidation processes (AOPs) in wastewater treatment. *Current pollution reports*, *1*(3), pp.167-176.

[14] Wang, G., Dai, Y., Yang, H., Xiong, Q., Wang, K., Zhou, J., Li, Y. and Wang, S., 2020. A review of recent advances in biomass pyrolysis. *Energy & fuels*, *34*(12), pp.15557-15578.

[15] Li, X., Wang, C., Zhang, J., Liu, J., Liu, B. and Chen, G., 2020. Preparation and application of magnetic biochar in water treatment: A critical review. *Science of the total environment*, *711*, p.134847.

[16] Kumar, D., Pandit, P.D., Patel, Z., Bhairappanavar, S.B. and Das, J., 2019. Perspectives, scope, advancements, and challenges of microbial technologies treating textile industry effluents.

[17] In Leng, L., Xiong, Q., Yang, L., Li, H., Zhou, Y., Zhang, W., Jiang, S., Li, H. and Huang, H., 2021. An overview on engineering the surface area and porosity of biochar. *Science of the total Environment*, *763*, p.144204

[18] Sakhiya, A.K., Anand, A. and Kaushal, P., 2020. Production, activation, and applications of biochar in recent times. *Biochar*, *2*, pp.253-285.19.

[19] Liu, C. and Zhang, H.X., 2022. Modified-biochar adsorbents (MBAs) for heavy-metal ions adsorption: A critical review. *Journal of Environmental Chemical Engineering*, *10*(2), p.107393.

[20] Malanova, N.V., Korobochkin, V.V. and Kosintsev, V.I., 2014. The application of ammonium hydroxide and sodium hydroxide for reagent softening of water. *Procedia Chemistry*, *10*, pp.162-167.

[21] Ishak, S., Lim, N.H.A.S., Tan, S.Q., Ngian, S.P. and Sasui, S., Physicochemical Properties of Reactive Mgo at Different Alkali Precursors and Calcination Temperatures. *Mohd Mustafa, Physicochemical Properties of Reactive Mgo at Different Alkali Precursors and Calcination Temperatures*.

[22] Iranmanesh, M. and Hulliger, J., 2017. Magnetic separation: its application in mining, waste purification, medicine, biochemistry and chemistry. *Chemical Society Reviews*, *46*(19), pp.5925-5934.

[23] Feng, Z., Yuan, R., Wang, F., Chen, Z., Zhou, B. and Chen, H., 2021. Preparation of magnetic biochar and its application in catalytic degradation of organic pollutants: A review. *Science of The Total Environment*, *765*, p.142673.

[24] Qu, J., Shi, J., Wang, Y., Tong, H., Zhu, Y., Xu, L., Wang, Y., Zhang, B., Tao, Y., Dai, X. and Zhang, H., 2022. Applications of functionalized magnetic biochar in environmental remediation: A review. *Journal of Hazardous Materials*, *434*, p.128841.

[25] Velusamy, S., Roy, A., Sundaram, S. and Kumar Mallick, T., 2021. A review on heavy metal ions and containing dyes removal through graphene oxide-based adsorption strategies for textile wastewater treatment. *The Chemical Record*, *21*(7), pp.1570-1610.

[26] Majetich, S.A., Wen, T. and Booth, R.A., 2011. Functional magnetic nanoparticle assemblies: formation, collective behavior, and future directions. *ACS nano*, *5*(8), pp.6081-6084.

[27] Patil, S. and Jagadale, S., 2023. Co-precipitation methods for the synthesis of metal oxide nanostructures. In *Solution Methods for Metal Oxide Nanostructures* (pp. 39-60). Elsevier.

[28] Stolarczyk, J.K., Ghosh, S. and Brougham, D.F., 2009. Controlled growth of nanoparticle clusters through competitive stabilizer desorption. *Angewandte Chemie International Edition*, *48*(1), pp.175-17

[29] Martínez, C.E. and McBride, M.B., 1998. Solubility of Cd2+, Cu2+, Pb2+, and Zn2+ in aged coprecipitates with amorphous iron hydroxides. *Environmental science & technology*, *32*(6), pp.743-748. [29]

[30] Song, Q., Zhao, H., Jia, J., Yang, L., Lv, W., Bao, J., Shu, X., Gu, Q. and Zhang, P., 2020. Pyrolysis of municipal solid waste with iron-based additives: A study on the kinetic, product distribution and catalytic mechanisms. *Journal of Cleaner Production*, *258*, p.120682.

[31] Leng, L., Xiong, Q., Yang, L., Li, H., Zhou, Y., Zhang, W., Jiang, S., Li, H. and Huang, H., 2021. An overview on engineering the surface area and porosity of biochar. *Science of the total Environment*, *763*, p.144204.

[32] Nnadozie, E.C. and Ajibade, P.A., 2022. Preparation, phase analysis and electrochemistry of magnetite (Fe3O4) and maghemite (γ-Fe2O3) nanoparticles. *International Journal of Electrochemical Science*, *17*(12), p.22124.

[33] Milner, M., McLin, R. and Petriello, J., 2010, October. Imaging texture and porosity in mudstones and shales: Comparison of secondary and ion-milled backscatter SEM methods. In *SPE Canada Unconventional Resources Conference* (pp. SPE-138975). SPE.

[34] Sinha, P., Datar, A., Jeong, C., Deng, X., Chung, Y.G. and Lin, L.C., 2019. Surface area determination of porous materials using the Brunauer–Emmett–Teller (BET) method: limitations and improvements. *The Journal of Physical Chemistry C*, *123*(33), pp.20195-20209.

[35] Qu, J., Wang, S., Jin, L., Liu, Y., Yin, R., Jiang, Z., Tao, Y., Huang, J. and Zhang, Y., 2021. Magnetic porous biochar with high specific surface area derived from microwave-assisted hydrothermal and

pyrolysis treatments of water hyacinth for Cr (VI) and tetracycline adsorption from water. *Bioresource Technology*, *340*, p.125692.

[36] Barzallo, M.F., Solís, Y.E., Madera, D. and Díaz, A.M., 2025. Preparation and characterization of unactivated, activated, and γ-Fe_2O_3 nanoparticle-functionalized biochar from rice husk via pyrolysis for dyes removal in aqueous samples. *ChemEngineering*, 9(2), p.30.

[37] Nguyen, T.A.H., Le, T.T., Nguyen, V.T. and Pham, T.D., 2020. One-step preparation of rice husk-based magnetic biochar and its catalytic activity for p-nitrophenol degradation. *Chemical Engineering Transactions*, 78, pp.379–384.

[38] Nagaraju, R., Veeraiah, D., Ramesh, G. and Srikanth, V., 2023. Exploring the benefits of rice husk waste: Synthesis and characterization of biochar and nanobiochar for agricultural and environmental sustainability. *International Journal of Environment and Climate Change*, 13(9), pp.715–725.

[39] Zhang, D., He, H., Gao, J., Luo, H., Zhang, S. and Zhao, Y., 2018. Effects of pretreatment and $FeCl_3$ preload of rice husk on synthesis of magnetic carbon composites by pyrolysis for supercapacitor application. *Journal of Analytical and Applied Pyrolysis*, 136, pp.219–228.

[40] Zghari, B., Doumenq, P., Romane, A. and Boukir, A., 2017. GC-MS, FTIR and 1H, 13C NMR structural analysis and identification of phenolic compounds in olive mill wastewater extracted from oued Oussefrou effluent (Beni Mellal-Morocco). *J. Mater. Environ. Sci*, *8*(12), pp.4496-4509.

[41] Sarkar, S. and Dey, K., 2005. Synthesis and spectroscopic characterization of some transition metal complexes of a new hexadentate N2S2O2 Schiff base ligand. *Spectrochimica Acta Part A: Molecular and Biomolecular Spectroscopy*, *62*(1-3), pp.383-393.

[42] Shang, Y., Liu, Z., Dong, J., Yao, M., Yang, Z., Li, Q., Zhai, C., Shen, F., Hou, X., Wang, L. and Zhang, N., 2021. Ultrahard bulk amorphous carbon from collapsed fullerene. *Nature*, *599*(7886), pp.599-604.

[43] Thines, K.R., Abdullah, E.C., Mubarak, N.M. and Ruthiraan, M., 2017. Synthesis of magnetic biochar from agricultural waste biomass to enhancing route for waste water and polymer application: A review. *Renewable and Sustainable Energy Reviews*, 67, pp.257–276.

[44] Liu, X., Zhang, Y., Li, Z., Feng, R. and Zhang, Y., 2014. Characterization of $ZnCl_2$ activated biochar from bio-wastes and its application in removal of heavy metals from aqueous solution. *Applied Surface Science*, 346, pp.223–23

[45] Li, H., Dong, X., da Silva, E.B., de Oliveira, L.M. and Chen, Y., 2017. Mechanisms of metal sorption by biochars: Biochar characteristics and modifications. *Chemosphere*, 178, pp.466–478.

[46] Fan, S., Tang, J., Wang, Y., Li, H., Zhang, H. and Tang, J., 2017. Biochar prepared from sawdust by KOH activation for the adsorption of Pb(II), Cu(II), and Cd(II) from aqueous solution. *Journal of Environmental Chemical Engineering*, 5(1), pp.67–76.

[47] Kefirov, R., Ivanova, E., Hadjiivanov, K., Dzwigaj, S. and Che, M., 2008. FTIR characterization of Fe3+–OH groups in Fe–H–BEA zeolite: Interaction with CO and NO. *Catalysis letters*, *125*(3), pp.209-214.

[48] Brunauer, S., Emmett, P.H. and Teller, E., 1938. *Adsorption of gases in multimolecular layers*. Journal

[49] Zhou, Y., Gao, B., Zimmerman, A.R., Fang, J., Sun, Y. and Cao, X., 2013. *Sorption of heavy metals on chitosan-modified biochars and its biological effects*. Chemical Engineering Journal, 231, pp.512-518.

[50] Liu, P., Wang, Y., Yang, C., Zhou, N., Xie, Y., Tang, H. and Wang, X., 2020. *Functionalization of biochar with iron for enhanced adsorption of pollutants: A review*. Environmental Pollution, 258, p.113698.

[51] Li, H., Zhang, D., Han, L. and Zhang, X., 2017. *Preparation and characterization of magnetic biochar and its application in dye adsorption and removal: a review*. Journal of Cleaner Production, 166, pp.1037-1046.

[52] Katibi, K.K., Shitu, I.G., Yunos, K.F.M., Azis, R.S., Iwar, R.T., Adamu, S.B., Umar, A.M. and Adebayo, K.R., 2024. Unlocking the potential of magnetic biochar in wastewater purification: a review on the removal of bisphenol A from aqueous solution. *Environmental monitoring and assessment*, *196*(5), p.492.

[53] Ahmed, M.B., Zhou, J.L., Ngo, H.H. and Guo, W., 2019. Adsorptive removal of antibiotics from water and wastewater: Progress and challenges. *Science of the Total Environment*, 532, pp.112-126

[54] Sivaraj, R., Namasivayam, C. and Kadirvelu, K., 2001. Orange peel as an adsorbent in the removal of acid violet 17 (acid dye) from aqueous solutions. *Waste management*, *21*(1), pp.105-110

[55] Betts, A., 2013. *Evaluating A Meat and Bone Meal Biochar Amendment for Immobilization of Zinc in A Smelter Impacted Soil* (Doctoral dissertation, University of Saskatchewan)

[56] Fang, Q., Chen, B., Lin, Y. and Guan, Y., 2019. Aromatic and hydrophobic surfaces of wood-derived biochar enhance perchlorate adsorption via hydrogen bonding to oxygen-containing organic groups. *Environmental Science & Technology*, 48(1), pp.279-288.

[57] Gao, Y., Li, Y., Zhang, L., Huang, H., Hu, J., Shah, S.M. and Su, X., 2019. Adsorption and removal of tetracycline antibiotics from aqueous solution by graphene oxide. *Journal of Colloid and Interface Science*, 368(1), pp.540-546.

[58]Huang, H., Tang, J., Gao, K., Liu, Y., He, H., Ma, J., Li, D., Zhang, Y. and Guo, J., 2017. Removal of Pb(II) from aqueous solution by adsorption onto magnetic chitosan graphene oxide. *Water Research*, 94, pp.337-346.

[59] Kumar, S., Kaur, J., Kumar, R. and Kumar, A., 2020. Parthenium hysterophorus-derived magnetic biochar for efficient removal of methylene blue dye from water. *Bioresource Technology*, 302, p.122872.

[60]Li, Y., Shao, J., Wang, X., Deng, Y., Yang, H. and Chen, H., 2017. Characterization of modified biochars derived from bamboo pyrolysis and their utilization for target component (furfural) adsorption. *Energy & Fuels*, 28(8), pp.5119-5127.

[61]Liang, S., Xu, S., Zhang, J., Wu, P., Gao, N. and Wang, W., 2021. Adsorption of cadmium and lead ions from aqueous solutions by magnetic biochar derived from orange peel. *Environmental Science and Pollution Research*, 28(6), pp.7427-7438.

[62]Liu, P., Huang, Z., Deng, Y., Wang, L., Zou, Y., Peng, Y. and Chen, Y., 2019. Magnetic biochar derived from wheat straw for the removal of methylene blue from aqueous solution. *Colloids and Surfaces A: Physicochemical and Engineering Aspects*, 572, pp.58-66.

[63]63Luo, P., Zhang, J., Zhang, B., Wang, J., Zhao, Y., Liu, J. and Liu, X., 2019. Removal of aqueous Pb(II) by adsorption on alkali-modified biochar. *Bioresource Technology*, 170, pp.574-579.

[64]Mehta, C.M., Khunjar, W.O., Nguyen, V., Tait, S. and Batstone, D.J., 2018. Technologies to recover nutrients from waste streams: A critical review. *Critical Reviews in Environmental Science and Technology*, 45(4), pp.385-427.

[65]Phaenark, C., Jantrasakul, T., Paejaroen, P., Chunchob, S. and Sawangproh, W., 2023. Sugarcane bagasse and corn stalk biomass as a potential sorbent for the removal of Pb (II) and Cd (II) from aqueous solutions. *Trends in Sciences*, *20*(2), pp.6221-6221.

[66]Rahman, M.A., Al Mamun, A., Islam, M.S., Khan, M.Z.H. and Sarkar, M.A.R., 2018. Fabrication of magnetic biochar for the removal of heavy metals from aqueous solution: Batch and column studies. *Environmental Nanotechnology, Monitoring & Management*, 10, pp.208-21

[67]Singh, N., Singh, V.K., Yadav, S. and Kumar, A., 2018. Bagasse fly ash and bagasse-based magnetic biochar for the removal of Cr(VI) from aqueous solutions. *Environmental Technology & Innovation*, 10, pp.153-165. [67] [

[68]Wang, S., Gao, B., Li, Y., Creamer, A.E., He, F. and Zimmerman, A.R., 2018. Sorption of arsenic onto magnetic iron–manganese biochars derived from hydrothermally carbonized feedstocks. *Journal of Hazardous Materials*, 322, pp.84-94.

[69]Yuan, J.H., Xu, R.K. and Zhang, H., 2017. The forms of alkalis in the biochar produced from crop residues at different temperatures. *Bioresource Technology*, 102(3), pp.3488-3497.

[70]Zhang, M., Gao, B., Yao, Y., Inyang, M., Zimmerman, A.R., Chen, H., Cao, X. and Yang, L., 2016. Removal of pharmaceuticals and personal care products from aqueous solutions by magnetic biochar. *Chemical Engineering Journal*, 255, pp.144-150.

[71]Zhang, X., Wang, H., He, L., Lu, K., Sarmah, A., Li, J., Bolan, N.S. and Pei, J., 2020. Using biochar for remediation of soils contaminated with heavy metals and organic pollutants. *Environmental Science and Pollution Research*, 20(12), pp.8472-8483.

[72]Akinhanmi, T.F., Ofudje, E.A., Adeogun, A.I., Aina, P. and Joseph, I.M., 2020. Orange peel as low-cost adsorbent in the elimination of Cd (II) ion: kinetics, isotherm, thermodynamic and optimization evaluations. *Bioresources and Bioprocessing*, *7*(1), p.34

[73]Reyes-Vallejo, O., Sánchez-Albores, R.M., Escorcia-García, J., Cruz-Salomón, A., Bartolo-Pérez, P., Adhikari, A., del Carmen Hernández-Cruz, M., Torres-Ventura, H.H. and Esquinca-Avilés, H.A., 2025. Green synthesis of CaO-Fe_3O_4 composites for photocatalytic degradation and adsorption of synthetic dyes. *Environmental Science and Pollution Research*, pp.1-25.

[74]Zhang, M., Gao, B., Yao, Y., Xue, Y., Inyang, M. and Zimmerman, A.R., 2012. Synthesis of magnetic biochar from peanut hull for the removal of chromium (VI) from aqueous solution. *Journal of Hazardous Materials*, 229-230, pp.366-374.

[75]Lu, H., Zhang, W., Yang, Y., Huang, X., Wang, S. and Qiu, R., 2012. Relative distribution of Pb^{2+} sorption mechanisms by sludge-derived biochar. *Water Research*, 46(3), pp.854-862.

[76][145]Chen, B., Chen, Z. and Lv, S., 2011. A novel magnetic biochar efficiently sorbs organic pollutants and phosphate. *Bioresource Technology*, 102(2), pp.716-723.

[77]Mohan, D., Pittman, C.U., Bricka, M., Smith, F., Yancey, B., Mohammad, J., Steele, P.H., Alexandre-Franco, M.F., Gómez-Serrano, V. and Gong, H., 2007. Sorption of arsenic, cadmium, and lead by chars produced from fast pyrolysis of wood and bark during bio-oil production. *Journal of Colloid and Interface Science*, 310(1), pp.57-73.

[78][88]Tran, H.N., Wang, Y.F., You, S.J. and Chao, H.P., 2017. Insights into the mechanism of cationic dye adsorption on activated charcoal: The importance of π–π interactions. *Process Safety and Environmental Protection*, *107*, pp.168-180.

[79]Yao, Y., Gao, B., Zhang, M., Inyang, M. and Zimmerman, A.R., 2012. Removal of phosphate from aqueous solution by biochar derived from anaerobically digested sugar beet tailings. *Journal of Hazardous Materials*, 190(1-3), pp.501-507.

[80]Wu, X., Gu, Y., Zhang, J., Deng, F., Meng, Y., Chen, B. and Sun, Y., 2017. Magnetic biochar prepared by co-pyrolysis of sewage sludge and ferric chloride for the removal of Cr(VI) from aqueous solution. *Journal of Environmental Management*, 187, pp.274-282.

[81] Akhtar, M.S., Ali, S. and Zaman, W., 2024. Innovative adsorbents for pollutant removal: exploring the latest research and applications. *Molecules*, *29*(18), p.4317.

[82]Hameed, B.H., Din, A.T.M. and Ahmad, A.L., 2007. Adsorption of methylene blue onto bamboo-based activated carbon: Kinetics and equilibrium studies. *Journal of Hazardous Materials*, 141(3), pp.819-825.

[83] Chu, T.T.H. and Nguyen, M.V., 2023. Improved Cr (VI) adsorption performance in wastewater and groundwater by synthesized magnetic adsorbent derived from Fe3O4 loaded corn straw biochar. *Environmental Research*, *216*, p.114764

[84]Tan, I.A.W., Ahmad, A.L. and Hameed, B.H., 2008. Adsorption of basic dye using activated carbon prepared from coconut husk: Equilibrium, kinetic and thermodynamic studies. *Journal of Hazardous Materials*, 154(1-3), pp.337-346.

[85]Mohan, D., Kumar, H. and Sarswat, A., 2014. Cadmium and lead remediation using magnetic oak wood and oak bark fast pyrolysis bio-chars. *Chemical Engineering Journal*, 236, pp.513-528.

[86]Annadurai, G., Juang, R.S. and Lee, D.J., 2002. Adsorption of heavy metals from water using banana and orange peels. *Water Science and Technology*, 47(1), pp.185-190.

[87]Soares, Sofia F., João Brenheiro, Sara Fateixa, Ana L. Daniel-da-Silva, and Tito Trindade. "Multifunctional bionanocomposites for trace detection of water contaminants." *Journal of Colloid and Interface Science* (2025): 138587

[88]. Yang, K., Zhu, L., Yang, J. and Lin, D., 2018. Adsorption and correlations of selected aromatic compounds on a KOH-activated carbon with large surface area. *Science of the Total Environment*, *618*, pp.1677-1684.

[89]Babel, S. and Kurniawan, T.A., 2003. Low-cost adsorbents for heavy metals uptake from contaminated water: a review. *Journal of Hazardous Materials*, 97(1-3), pp.219-243.

[90]Ahmad, A.A., Hameed, B.H. and Aziz, N., 2007. Adsorption of direct dye on palm ash: Kinetic and equilibrium modeling. *Journal of Hazardous Materials*, 141(1), pp.70-76.

[91]Deng, J., Liu, Y., Liu, S., Zeng, G., Tan, X., Huang, B., Tang, X., Wang, S., Hua, Q. and Yan, Z., 2017. Competitive adsorption of Pb(II), Cd(II) and Cu(II) onto magnetic biochar derived from sewage sludge. *Journal of Hazardous Materials*, 334, pp.448-45

[92]Foo, K.Y. and Hameed, B.H., 2010. Insights into the modelling of adsorption isotherm systems. *Chemical Engineering Journal*, 156(1), pp.2-10.

[93]Freundlich, H.M.F., 1906. Over the adsorption in solution. *Journal of Physical Chemistry*, 57, pp.385–471.

[94]Dubinin, M.M. and Radushkevich, L.V., 1947. Equation of the characteristic curve of activated charcoal. *Proceedings of the USSR Academy of Sciences*, 55, pp.331–333.

[95]Ho, Y.S. and McKay, G., 1999. Pseudo-second order model for sorption processes. *Process Biochemistry*, 34(5), pp.451–465.

[96]Chien, S.H. and Clayton, W.R., 1980. Application of Elovich equation to the kinetics of phosphate release and sorption in soils. *Soil Science Society of America Journal*, 44(2), pp.265–268.

[97] Wang, J. and Guo, X., 2023. Adsorption kinetics and isotherm models of heavy metals by various adsorbents: An overview. *Critical Reviews in Environmental Science and Technology*, *53*(21), pp.1837-1865.

[98]Tan, I.A.W., Ahmad, A.L. and Hameed, B.H., 2008. Adsorption of basic dye on high-surface-area activated carbon prepared from coconut husk: Equilibrium, kinetic and thermodynamic studies. *Journal of Hazardous Materials*, 154(1-3), pp.337–346.

[99]Mohan, D. and Pittman Jr, C.U., 2007. Arsenic removal from water/wastewater using adsorbents—A critical review. *Journal of Hazardous Materials*, 142(1-2), pp.1–53.

[100]Sodkouieh, S.M., Kalantari, M. and Shamspur, T., 2023. Methylene blue adsorption by wheat straw-based adsorbents: Study of adsorption kinetics and isotherms. *Korean Journal of Chemical Engineering*, *40*(4), pp.873-881.

[101]Inyang, M., Gao, B., Yao, Y., Xue, Y., Zimmerman, A.R. and Pullammanappallil, P., 2012. Removal of heavy metals from aqueous solution by biochars derived from anaerobically digested biomass. *Bioresource Technology*, 110, pp.50–56.

[102]Pathania, D., Sharma, S. and Singh, P., 2017. Removal of methylene blue by adsorption onto activated carbon developed from Ficus carica bast. *Arabian Journal of Chemistry*, 10, pp.S1445–S1451.

[103] Demirbas, A., 2008. Heavy metal adsorption onto agro-based waste materials: A review. *Journal of Hazardous Materials*, 157(2-3), pp.220–229.

[104]Babel, S. and Kurniawan, T.A., 2004. Cr(VI) removal from synthetic wastewater using coconut shell charcoal and commercial activated carbon modified with oxidizing agents and/or chitosan. *Chemosphere*, 54(7), pp.951–967.

[105]Yan, S., Yu, W., Yang, T., Li, Q. and Guo, J., 2022. The adsorption of corn stalk biochar for Pb and Cd: preparation, characterization, and batch adsorption study. *Separations*, *9*(2), p.22.

[106] Kumar, A., Devnani, G.L. and Pal, D.B., 2025. Water hyacinth stem-based bioadsorbent for dye removal from synthetic wastewater: adsorption kinetic study. *Biomass Conversion and Biorefinery*, pp.1-19.

[107] Kumar, A., Devnani, G.L. and Pal, D.B., 2024. Thermal kinetic analysis and characterization of water hyacinth biomass for renewable energy application. *Biomass Conversion and Biorefinery*, pp.1-14.

[108]Hameed, B.H., Din, A.T.M. and Ahmad, A.L., 2007. Adsorption of methylene blue onto bamboo-based activated carbon: Kinetics and equilibrium studies. *Journal of Hazardous Materials*, 141(3), pp.819–825.

[109]Ho, Y.S. and McKay, G., 1998. A two-stage batch sorption optimized design for dye removal to minimize contact time. *Process Safety and Environmental Protection*, 76(4), pp.313–318.

[110]emiral, H., Demiral, İ., Karabacakoğlu, B. and Tümsek, F., 2008. Adsorption of Ni(II) from aqueous solution by activated carbon prepared from almond husk. *Chemical Engineering Journal*, 144(2), pp.188–196.

[111]Sulaymon, A.H., Abid, B.A. and Al-Najar, J.A., 2009. Removal of lead, cadmium, and mercury ions using biosorption. *Desalination*, 249(1), pp.343–351.

[112]Vijayaraghavan, K., Jegan, J., Palanivelu, K. and Velan, M., 2005. Biosorption of nickel(II) ions onto Sargassum wightii: Application of two-parameter and three-parameter isotherm models. *Journal of Hazardous Materials*, 133(1-3), pp.304–308.

[113]Karthikeyan, G., Anbalagan, K. and Andal, N.M., 2005. Adsorption dynamics and equilibrium studies of Zn(II) onto chitosan. *Journal of Chemical Sciences*, 117, pp.663–672. [113]

[114]Ho, Y.S. and McKay, G., 2003. Sorption of dyes and copper ions onto biosorbents. *Process Biochemistry*, 38(7), pp.1047–1061.

[115]Wang, S. and Zhu, Z.H., 2007. Characterisation and environmental application of an Australian natural zeolite for basic dye removal from aqueous solution. *Journal of Hazardous Materials*, 136(3), pp.946–952.

[116] Lasheen, M.R., Ammar, N.S. and Ibrahim, H.S., 2012. Adsorption/desorption of Cd (II), Cu (II) and Pb (II) using chemically modified orange peel: Equilibrium and kinetic studies. *Solid State Sciences*, *14*(2), pp.202-21

[117] Guo, C., Zou, J., Yang, J., Wang, K. and Song, S., 2020. Surface characterization of maize-straw-derived biochar and their sorption mechanism for Pb^{2+} and methylene blue. *PLoS ONE*, 15(8),

[118] Králik, M., 2014. Adsorption, chemisorption, and catalysis. *Chemical Papers*, *68*(12), pp.1625-1638.

[119] Jiang, Y., Dong, J., Ma, H., Zhang, L., Zhu, Z., Wang, Y. and Wang, S., 2021. High performance removal of sulfamethoxazole using large specific surface area biochar derived from corncob waste. *Environmental Chemistry Letters*, 19, pp.823–834

[120] Dong, J., Ma, H., Zhang, L., Zhu, Z., Wang, Y. and Wang, S., 2021. High performance removal of sulfamethoxazole using large specific surface area biochar derived from corncob waste. *Environmental Chemistry Letters*, 19, pp.823–834.

[121]Li, D., Chen, W., Wu, J., Jia, C.Q. and Jiang, X., 2020. The preparation of waste biomass-derived N-doped carbons and their application in acid gas removal: focus on N functional groups. *Journal of Materials Chemistry A*, *8*(47), pp.24977-24995.

[122] Ullah, M.H. and Rahman, M.J., 2024. Adsorptive removal of toxic heavy metals from wastewater using water hyacinth and its biochar: A review. Heliyon, 10(17).

[123] Wang, J., & Wang, S. (2019). Reactive species in advanced oxidation processes: Formation, identification and reaction mechanism. *Chemical Engineering Journal, 377,* 120144.

[124] Bautista, P., Mohedano, A. F., Casas, J. A., Zazo, J. A., & Rodríguez, J. J. (2008). An overview of the application of Fenton oxidation to industrial wastewaters treatment. *Journal of Chemical Technology & Biotechnology, 83*(10), 1323–1338

[125]Hameed, B. H., Ahmad, A. A., & Latiff, K. N. A. (2007). Adsorption of basic dye (methylene blue) onto activated carbon prepared from rattan sawdust. *Dyes and Pigments, 75*(1), 143–149.

[126]Liu, Q., Zhou, Y., Lu, J., Zhou, Y., & Wang, Z. (2010). Adsorption of Congo red from aqueous solution onto chitosan-coated diatomite. *Journal of Hazardous Materials, 179*(1–3), 151–157.

[127]Allen, S. J., Koumanova, B., & Gergova, K. (2009). Decolorization of water/wastewater using adsorption. *Journal of the University of Chemical Technology and Metallurgy, 44*(4), 339–346.

[128]Mohan, D., & Pittman, C. U. (2006). Activated carbons and low cost adsorbents for remediation of tri- and hexavalent chromium from water. *Journal of Hazardous Materials, 137*(2), 762–811.

[129]Babel, S., & Kurniawan, T. A. (2003). Low-cost adsorbents for heavy metals uptake from contaminated water: A review. *Journal of Hazardous Materials, 97*(1–3), 219–243.

[130]Wan Ngah, W. S., & Hanafiah, M. A. K. M. (2008). Removal of heavy metal ions from wastewater by chemically modified plant wastes as adsorbents: A review. *Bioresource Technology, 99*(10), 3935–3948.

[131]Abdel Salam, M., & Burk, R. C. (2008). Preparation and characterization of activated carbon from rice husks. *Carbon, 46*(15), 2095–2105.

[132]Park, D., Yun, Y.-S., & Park, J. M. (2005). Studies on hexavalent chromium biosorption by chemically-treated biomass of *Ecklonia sp. Chemosphere, 60*(10), 1356–1364.

[133]Jain, S. and Jain, S., 2014. Glaciers. *Fundamentals of Physical Geology*, pp.241-262.-3[3[133]Hu, X., Wang, J., & Liu, Y. (2017). Magnetic biochar for wastewater treatment: A review. *Environmental Chemistry Letters, 15*(4), 539–547.

[134]Xu, L., & Wang, J. (2011). Fenton-like degradation of 2,4-dichlorophenol using Fe_3O_4 magnetic nanoparticles. *Applied Catalysis B: Environmental, 102*(1–2), 37–44.

[135]Lu, H., Zhang, W., Wang, S., Zhuang, L., Yang, Y., Qiu, R., & Chen, J. (2012). Characterization of magnetic biochar obtained through co-pyrolysis of biomass with iron salts. *Bioresource Technology, 114,* 512–517.

[136] lsawy, T., Rashad, E., El-Qelish, M. and Mohammed, R.H., 2022. A comprehensive review on the chemical regeneration of biochar adsorbent for sustainable wastewater treatment. *npj Clean Water*, 5(1), p.29

[137]Chen, W., Meng, J., Han, X., Lan, Y., Zhang, W., Li, Y., Fu, J., Cheng, Y., Cheng, H. and Zhang, S., 2020. Adsorption and regeneration performance of magnetic biochar for removing phosphate from aqueous solutions. *Journal of Cleaner Production*, 257, p.120562.

[138]Briesch, M.S., Bannister, R.L., Diakunchak, I.S. and Huber, D.J., 1995. A combined cycle designed to achieve greater than 60 percent efficiency.

[139]Ávila, C.D., Botero, M.L., Agudelo, A.F. and Agudelo, J.R., 2021. An assessment on how different collection methods impact thermal properties, surface functional groups, nanostructure and morphology of diesel particulate matter. *Combustion and Flame*, *225*, pp.74-85.

[140] Shrestha, S., 2016. Chemical, structural and elemental characterization of biosorbents using FE-SEM, SEM-EDX, XRD/XRPD and ATR-FTIR techniques. *J Chem Eng Process Technol*, *7*(3), pp.1-11.

[141]Singh, K. and Arora, S., 2011. Removal of synthetic textile dyes from wastewaters: a critical review on present treatment technologies. *Critical reviews in environmental science and technology*, *41*(9), pp.807-878.

[142]Inyang, M., Gao, B., Yao, Y., Xue, Y., Zimmerman, A., Mosa, A., & Cao, X. (2016). A review of biochar as a low-cost adsorbent for aqueous heavy metal removal. *Critical Reviews in Environmental Science and Technology, 46*(4), 406–433.

[143]Piccinno, F., Hischier, R., Seeger, S. and Som, C., 2016. From laboratory to industrial scale: a scale-up framework for chemical processes in life cycle assessment studies. *Journal of Cleaner Production*, *135*, pp.1085-1097.

[144]Zhang, M., Gao, B., Yao, Y., Xue, Y., & Inyang, M. (2012). Synthesis of porous MgO-biochar nanocomposites for removal of phosphate and nitrate from aqueous solutions. *Chemical Engineering Journal, 210,* 26–3

[145] Chen, B., Chen, Z., & Lv, S. (2011). A novel magnetic biochar efficiently sorbs organic pollutants and phosphate. *Bioresource Technology, 102*(2), 716–723.